Axon diameter mapping in crossing fibers with diffusion MRI

Hui Zhang[1], Tim B Dyrby[2], and Daniel C Alexander[1]

[1]*Department of Computer Science & Centre for Medical Image Computing, University College London, London, United Kingdom,* [2]*Danish Research Center for Magnetic Resonance, Copenhagen University Hospital, Hvidovre, Denmark*

INTRODUCTION This work presents a technique for mapping axon diameter in regions of crossing fibers. Direct measurement of microstructure, such as axon diameter and density, provides more specific information about the role and performance of white matter (WM) pathways than diffusion-tensor imaging. A particularly successful approach, exemplified by [1,2], is the model-based strategy in which a geometric model of the microstructure of interest predicts the MR signal from water diffusing within. In estimating axon diameters, previous methods assume WM models with only a single dominant orientation. The AxCaliber technique by Assaf et al [3,4] and the ActiveAx technique by Alexander et al [5,6] assume a model of *single* axon orientation. The ActiveAx was recently extended to account for the presence of axons with *dispersed* orientations [7]. Although it enables axon diameter mapping for a much broader range of WM areas, it still is valid *only* for regions with a *single dominant* orientation. Regions with crossing fibers are widespread in the brain [8] and a solution to this problem is prerequisite to realizing whole-brain axon diameter mapping. We address this problem by extending the ActiveAx with a crossing-fiber model that supports the simultaneous estimation of crossing configuration and microstructure features. We demonstrate the feasibility of our approach with both synthetic and *ex vivo* brain imaging data.

METHODS Tissue and signal model: The proposed crossing-fiber model represents WM as one or more populations of axons embedded in a homogeneous medium. Each axon population is modeled separately with the minimal model of white matter diffusion (MMWMD) [6]. Specifically, the volume fractions of the intracellular compartment (IC) and extracellular compartment (EC) are v_{ic} and $(1-v_{ic})$, respectively. The IC and EC signals, A_{ic} and A_{ec}, are computed as the weighted sums of the respective signals from individual axon populations, weighted by their respective relative volume fractions. The IC and EC signals of the i-th axon population are determined with MMWMD using its relative volume fraction f^i_{ic}, its single diameter, a_i, and its orientation $\mathbf{n}_i$. MMWMD includes an additional isotropic restricted (IR) compartment to account for observed restrictions parallel to axons with the signal $A_{ir}=1$ and a volume fraction of v_{ir}. Parameter estimation: We employ the robust three-stage fitting procedure in [6] to estimate the parameters of the crossing-fiber model from the MR signal. It involves an initial grid search, a subsequent maximum-likelihood estimation using gradient-descent, and finally a global fitting using Markov chain Monte Carlo (MCMC). We adopt the MCMC settings in [6]: 40 samples at intervals of 200 iterations after a burn-in of 2000 iterations. Ex vivo Imaging: We acquired diffusion imaging data of a 32-month perfusion-fixed Vervet monkey on a pre-clinical 4.7T Varian system with maximum gradient strength of 400 mT/m. The protocol is determined with the experimental design optimization in [5]. It consists of three HARDI shells: number of gradient directions = [103, 106, 80], δ = [5.6, 7.0, 10.5] ms, Δ = [12, 20, 17] ms, |G| = [300, 210, 300] mT/m, corresponding to b = [2084, 3084, 9550] s/mm^{-2}. Additional imaging parameters are as follows: 30 sagittal slices about the midsagittal plane, matrix size 128x256, voxel size 0.5x0.5x0.5 mm^3, TE=36ms, TR=2500ms, single-line spin-echo readout, SNR at b=0 about 20. Monte Carlo simulation: We use the Monte-Carlo diffusion simulator in Camino [10] to generate synthetic MR data from a broad set of two-fiber crossing substrates. The simulated acquisition uses the ex vivo protocol and adds Rician noise to match the SNR of the ex vivo data. The set of true substrate parameters are 1) v_{ic} = 0.7, 2) the axon diameter combinations = {{2,2}, {2,4}, {2,6},{4,4},{4,6}, {6,6}} µm, 3) f^1_{ic} = {0.3,0.5,0.7} (for two-fiber crossing: $f^2_{ic} = 1-f^1_{ic}$), 4) crossing angles varying from 30° to 90° in 15° increment. To avoid possible orientation dependence, 20 different instances of each configuration are created with random 3-D rotations applied to the initial configuration. Camino does not simulate the IR compartment, thus v_{ir} = 0. *Region-of-interest*: We manually define a region-of-interest (ROI) with known fiber crossing to assess the efficacy of the crossing-fiber model in the ex vivo data. The interface between the corpus callosum and the cingulum bundle (Fig 1) is chosen in particular, because it is a well-defined 90° two-fiber crossing and can be clearly identified on the FA map as a dark band flanked by the voxels with high FA (Fig 1). The ROI includes both the interface and a layer of the flanking voxels on each side.

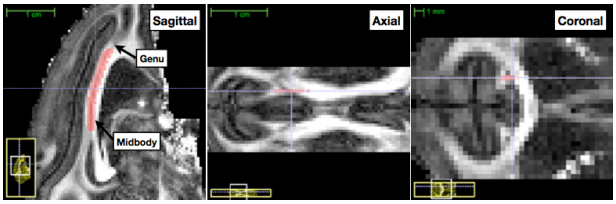

Fig 1: Crossing region-of-interest between the corpus callosum and the cingulum

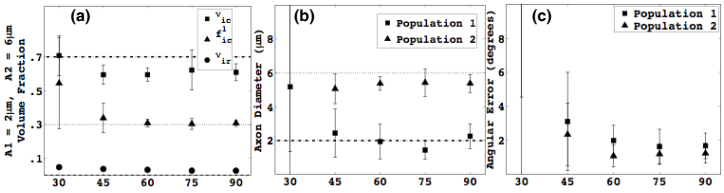

Fig 2: For illustration, the example parameter estimates for the synthetic substrate: {2,6} µm, f^1_{ic} = 0.3, and all the crossing angles (the horizontal axis).

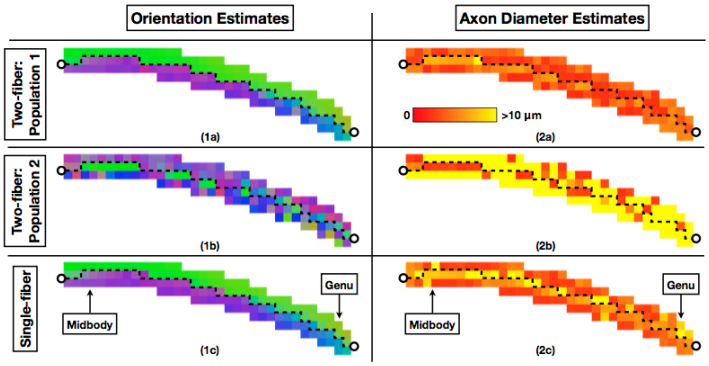

Fig 3: Parameter estimates for the ex vivo data using both the two-fiber and single-fiber models

EXPERIMENTS & RESULTS Synthetic data: We use the data from Monte Carlo simulation to assess the accuracy and precision of the microstructure estimates with respect to known ground truths. The results show that, for crossing angles larger than 45°, the two-fiber model is able to both resolve the crossing fiber configuration and estimate microstructure features: 1) The mean angular errors for both orientations are below 5° (Fig 2c). 2) The diameters of both axon populations can be estimated and differentiated from one another (Fig 2b). 3) The volume fractions f^1_{ic} and v_{ir} are estimated accurately and v_{ic} is slightly underestimated (Fig 2a). Ex vivo data: We compare the voxel-wise parameter estimates for the defined ROI (Fig 1) from the two-fiber model to the ones from the single-fiber model (Fig 4). The key result is that, for the voxels at the interface, only the two-fiber model provides sensible axon diameter estimates. Observe that the axon diameter estimates from the single-fiber model are 10µm or higher around the interface, significantly higher than 2µm, the value found in the histology literature [11]; they are sensible only for the surrounding voxels without fiber crossing (Fig 4.2c). In contrast, the estimates from the two-fiber model, for the voxels at the interface, are about 2µm for both fiber populations (Fig 4.2a-2b); for the surrounding voxels, only one population has an estimate about 2µm while the other has an estimate that indicates the absence of this population, i.e., the voxel has only a single fiber population (Fig 4.2a-2b). (40µm is the maximum value allowed in our fitting routine to indicate the negligible presence of the corresponding axon population). In addition, the results demonstrate that the two-fiber model provides sensible orientation estimates for both axon populations (Fig 4.1a-1b). The orientations are either along the cingulum bundle (green) or along the corpus callosum (blue), consistent with known anatomy.

DISCUSSION We demonstrate that the proposed crossing-fiber model is able to both resolve the configuration of fiber crossing and establish the microstructure characteristic of each axon population at the crossing. Furthermore, we show that for fiber crossing regions, assuming a single-fiber model leads to overestimation of axon diameters even for the dominant axon population. Considering the difficulty in estimating axon diameter for regions with a single orientation, it is both remarkable and encouraging that the proposed method enables the estimation of axon diameter for at least one of the crossing fiber populations. The current study considers only the more common crossing configuration due to partial volume. Future work will examine configurations with interdigitated crossing fibers. We will also evaluate the feasibility of this approach for in vivo imaging data and extend the model to describe multimodal orientation distributions with dispersion.

ACKNOWLEDGEMENT The future and emerging technologies (FET) program of the EU FP7 framework funds the CONNECT consortium and supports this work.

REFERENCE 1. Stanisz et al, MRM 97; 2. Assaf et al, MRM 04; 3. Assaf et al, MRM 08; 4. Barazany et al, BRAIN 09; 5. Alexander, MRM 08; 6. Alexander et al, NIMG 10; 7. Zhang et al. NIMG 11; 8. Seunarine and Alexander. Diffusion MRI 09; 9. Murday et al. J Chem Phys 68; 10. Cook et al. ISMRM 06; 11. Lamantia and Rakic. J Comp Neurol 90.